Mysterious Negative Velocity Profile in a Miniaturized Velocity Profile Interrogator Solved Remotely

Nina T. Jones, Sean R. Niemi, and Matthew J. Traum
University of Florida/University of Florida/Engineer Inc.

Abstract

This work's overall objective is to report a hands-on fluid dynamics teaching lab kit shippable to students taking lab-intensive remote MAE courses. This paper describes a prototype small-scale wind tunnel kit anchoring this application. Tunnel velocity profile characterization by pitot-static probe revealed an unexpected negative velocity profile initially attributed to recirculation. The cause was ultimately diagnosed as vorticity using a ping pong ball for inexpensive flow visualization. These impacts were minimized by addition of screen meshes and/or a metal honeycomb upstream. Ultimately, honeycomb provided the best flow correction as it most closely reflected the theoretical $1/7^{th}$ power law. The experiment also demonstrates entry length theory as the velocity profile is observed developing at greater tunnel axial lengths.

Keywords

hands-on laboratory kits, velocity profile, remote learning, hybrid teaching, flow correction

Introduction

Nearly all undergraduate engineering courses, including laboratories, were moved online in the fall of 2020 due to COVID-19. As no fully online ABET-accredited mechanical engineering bachelor's degree programs yet exist[1], a key challenge was porting applied hands-on laboratory experiences to the remote learning environment while providing students with experiences as pragmatic and engaging as standard brick-and-mortar laboratories[2]. Faculty have tried various creative methods for remote lab instruction[2], and one approach to maintaining experiential learning in spite of the pandemic was sending kits by mail to students.

This paper reports development of a hands-on laboratory teaching kit that can be shipped to students taking fluid mechanics remotely. Recipients unbox the kits, build the experiments, collect and analyze data, and discuss results with online peers and instructors just as their counterparts would do in face-to-face teaching labs. Care is exercised in kit design to ensure no loss of fidelity in observing or measuring engineering phenomena of interest. Another crucial kit attribute is modularity – the ability to run multiple experiments with the same set of components. Modular kits enable students to conduct different experiments and observe/measure a variety of phenomena without significantly increasing kit cost.

The lab kit contains an apparatus allowing students to characterize velocity profiles for various cylindrical pipe configurations. The kit reinforces and expands upon pipe flow theory introduced

in the classroom. This paper addresses the challenges overcome in characterizing the initial prototype and notes anecdotally the important student learning that occurred while performing this work remotely.

Background Information

Since the 1990s, distance learning through the Internet has come to the forefront of higher education. While fields such as the humanities, social and behavioral sciences, business, and management have led this charge, engineering education was later in moving toward online delivery methods[4]. Online education is shown to match or exceed traditional face-to-face education with benefits including 1) increased accessibility, 2) increased retention and completion, 3) increased flexibility, and 4) increased interaction and engagement. A major challenge for the field of engineering stems from incorporation of laboratory and design components critical to post-graduation student performance in the workforce[2].

There exist three main types of teaching laboratories: on-site, virtual, and remote. On-site laboratories were the most common pre-COVID, but they are currently problematic because of pandemic health concerns. Virtual laboratories by contrast cannot spread COVID, but they have many pedagogical drawbacks. Remote laboratories provide the best of both worlds offering students a pragmatic and safe experience. In fact, the literature shows that students can favor these remote lab experiences over on-site laboratories[4,5].

In one example measuring student attitudes and performance under all three laboratory scenarios, Corter and colleagues explored student achievement of learning objectives using cantilever beam experiments where content was delivered in three different environments: 1) brick-and-mortar labs, 2) lab kits at home, and 3) remote labs via computer simulation. These researchers found that at home, hands-on experiments were at least as effective as traditional brick-and-mortar labs for student learning. Moreover, student survey responses favored the remote lab experiences and remote students performed better in outcome achievement[6,7]. Investigations employing lab kits in other engineering disciplines agree with conclusions of Corter and others that remote hands-on experiments are better for student learning than traditional labs. The results suggest that each student gains experience building and running their own experiments, and they can explore interesting or unexpected observations at will without the time constraint of a classroom lab schedule[8]. Further benefits include the ability for experiments to be tailored by the teacher to meet student needs and the ability of laboratories to be readily shared between universities[9].

Just as important, there is growing need for remote engineering practice as industry has increasingly turned to remote and virtual laboratories. Many reasons underpin this trend including increased complexity of tasks, increased cost of equipment and software coupled with short term project time frames, the necessity of trained advanced equipment operators, and the globalization of labor. Remote laboratories have been found to be a benefit because they allow instrumentation and test results to be shared between employees at different locations or even between companies, and long-term experiments can be supervised from home or an office. Thus, it is desirable for students to be trained for this online setting by providing relevant online engineering learning experiences, particularly laboratories[4].

Theory

Pipe flow is classified as internal flow, where fluid is constrained by the walls of the pipe and flow is driven by a pressure gradient. The Reynolds number, Re_D, predicts flow behavior under various conditions. It is a ratio between inertial and viscous forces, where the diameter, D, average fluid velocity, U_{avg}, and kinematic velocity, ν, are needed to perform calculations.

$$Re_D = \frac{U_{avg} D}{\nu} \ldots (1)$$

The Reynolds number dictates whether flow is in the laminar or turbulent regime. In the laminar regime, streamlines are flat allowing flow to be smooth and orderly. In the turbulent regime, flow fluctuates and is disorderly: the regime is most reflective of practical flow[10,11]. When the Reynold's number is less than the critical Reynolds number, $Re_{D,crit}$, flow is laminar, and when it is greater than the critical Reynolds number, the flow is transitional or turbulent[12].

$$Re_{D,crit} = 2300 \ldots (2)$$

For both regimes, there is an axial pipe length up to which flow velocity profile is developing, referred to as the entrance length, L_e, and following this point the flow becomes fully developed (Fig. 1). This length is based upon the merging of developing boundary layers in which viscous effects impact flow[11]. The velocity profile remains constant in the fully developed flow region, and for turbulent flow, this profile shape follows the theoretical 1/7th Power Law[13].

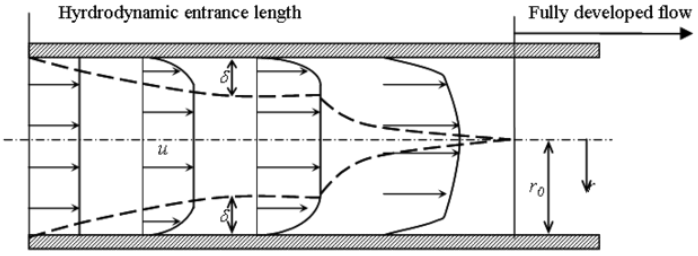

Fig. 1. Turbulent velocity profile development in a circular pipe of radius, r_o[14].

For turbulent flow, the entrance length can be calculated if both the Reynolds number and pipe diameter are known[15].

$$L_{e,turbulent} = 4.4 D Re_D^{1/6} \ldots (3)$$

Pitot-static probes are instruments that take local differential pressure readings in a flow field. They are often used to measure aircraft velocities or for wind tunnel characterization, as is the case here. The probe consists of a tube with a hole through its central axis as well as several holes in the face radially outward. This configuration allows total pressure, P_t, and static pressure, P_s, to be simultaneously monitored[16]. The difference between these values yields dynamic pressure, which determines local velocity, U, at the point of measurement using Bernoulli's Equation (4). This equation applies conservation of energy principles and assumes flow along a horizontal streamline is inviscid, steady, and incompressible[17].

$$P_s + \frac{\rho_{air} U^2}{2} = P_t \ldots (4)$$

Apparatus Description

The approach to creating a lab kit to illuminate pipe flow was shrinking a brick-and-mortar experiment, eliminating needless complexity and cost to achieve kits scaled for inexpensive mailing to remote learners. Shown schematically in Fig. 2, the apparatus measures internal pipe flow velocity profile shapes by rastering a pitot-static probe across the opening of a pipe with fan air forced through. It is essentially a miniaturized wind tunnel, mimicking equipment often found in standard mechanical or aerospace engineering laboratories. The deconstructed apparatus fits in a 40-quart shipping container and has a total material cost of ~$250.

Fig. 2. Velocity profile interrogator kit setup reflecting the conditions a remote learner may experience.

The interrogator's main structure consists of two coupled lengths of 100-mm-ID diameter PVC sewer pipe, allowing a total pipe length of 1-meter. Four u-bolt muffler clamps, two per each half-meter pipe section, provide mechanical stability to rest on a flat surface.

The fan driving flow in the pipe is a 120 mm x 120 mm variable speed computer fan where desired fan velocity is set via a voltage controller. The fan is fastened to a 100-mm-OD fan duct allowing it to be joined with the pipe.

The pitot probe manual rastering mechanism is built around a steel caliper. This caliper is mounted to the table with a table vice clamp so the direction of motion of the free-moving caliper jaw is perpendicular to the pipe's central axis. This jaw is tapped and fastened with a 3-inch bolt. The pitot-static probe is mounted to this bolt between two nuts at a height allowing the pipe's largest diameter to be investigated. Finally, the probe's ports are connected via silicon tubing to a digital manometer so differential pressure measurements can be taken.

Methods

Experimentation to characterize this system was conducted in a remote location by the lead author, an undergraduate mechanical engineering senior, to mimic conditions a remote learner might face. The prototype kit was mailed to the student experimenter who constructed all experiments and collected data in physical isolation.

Data collection was conducted for the setup (Fig. 2) with the maximum voltage supplied to the fan. The probe was rastered across the pipe's full open diameter with measurements taken at 1 mm increments, with incrementation controlled manually via adjustment of the caliper and observing its digital callout. The measurements taken at each point included maximum, minimum and average manometer readings.

Data collection was repeated for five further apparatus configurations. Directly downstream of the fan, where the fan was fastened to the duct, additional components could be added (Fig. 3). Namely, one, two, and three screen meshes were introduced and investigated. For the remaining two configurations, a 1/2-inch thick aluminum honeycomb was introduced. Investigation was carried out at the full 1-meter pipe length, as was the case for all other configurations and also for 1/2-meter pipe length.

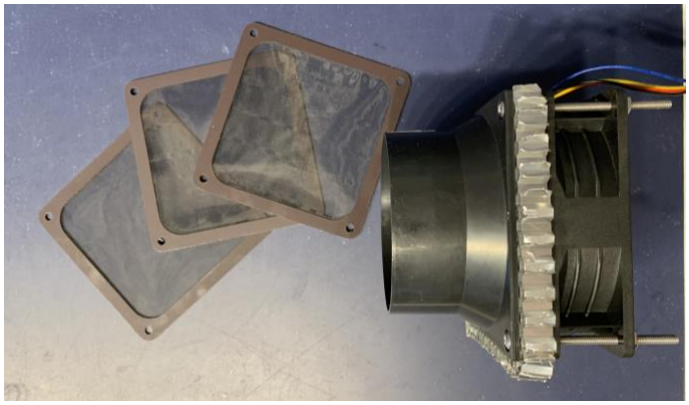

Fig. 3. Duct and fan assembly that can be rearranged to include meshes or a honeycomb.

Finally, the full 1-meter-long system was arranged vertically, with the fan parallel to the ground, and the open diameter facing the ceiling. A ping pong ball was introduced for flow visualization when the setup included one, two and three meshes as well as the honeycomb, and observations were noted.

Results

Manometer readings were converted to velocity for each collected data point. These readings were taken in inches of water and first converted to dynamic pressure in lbf/ft^2.

$$P_t - P_s = \rho_{H_2O} g h \ldots (5)$$

This dynamic pressure was then used to solve for velocity from (Eq. 4) and converted from ft/s to

m/s. For these calculations, gravity was taken as 32.17 ft/s^2, the density of water, ρ_{H_2O}, was taken as 1.94 slug/ft^3, and the density of air, ρ_{air},was taken as 0.002329 slug/ft^3. Density values corresponded to 68 °C [20 °C].

For each of the six total configurations where data were collected across the full pipe diameter, the average velocity, Reynolds Number (Eq. 1), and entrance length (Eq. 3) were calculated (Table I). For every case, the flow regime was classified as turbulent (Eq. 2).

TABLE I
DATA ANALYSIS FOR FLOW SET UPS

Configuration	Average Velocity (m/s)	Reynolds Number	Entrance Length (m)
No Meshes	2.04	13666	2.19
One Mesh	1.78	11951	2.14
Two Meshes	5.52	37021	2.58
Three Meshes	5.48	36715	2.58
Honeycomb (1 m)	9.65	64701	2.83
Honeycomb (1/2 m)	8.88	59489	2.79

There were five apparatus configurations for which data were collected across the full pipe diameter with a total pipe length of 1 meter. These configurations included no meshes or honeycomb, one mesh, two meshes, three meshes and one metal honeycomb. For each, velocity versus diametral probe position was plotted (Figs. 4-8).

With no meshes or honeycomb (Fig. 4), there was a “dead spot” in the center of the flow field. The impact could be observed for a span of 61 mm, determined by a shift to a negative slope when analyzing data from the pipe walls to its central axis. In this dead spot the pitot-static probe registered negative velocity readings, with a minimum reading of -8.15 m/s and average of 2.04 m/s. Upon introduction of a single mesh (Fig. 5), the dead spot and negative velocity readings were still present, but they were reduced with a minimum reading of -5.76 m/s. Furthermore, the average velocity, 1.78 m/s was lower than without the mesh. Upon introduction of two meshes (Fig. 6), the dip in the center of the flow field was still apparent, yet much less prominent as compared to the first two configurations. The minimum reading of 0 m/s occurred central to the distribution. Further, the average velocity of 5.52 m/s was more than double the previous two configuration average velocities. Upon introduction of three meshes (Fig. 7), this dead spot was almost entirely mitigated with a minimum reading of 4.51 m/s occurring central to the distribution, higher than any of the previous configurations. This minimum was closest in value to that of its average velocity, 5.48 m/s, which was just shy of mean velocity associated with two meshes. Finally, upon introduction of a metal honeycomb (Fig. 8), the dead spot was nonexistent, with the minimum reading of 7.34 m/s occurring at the walls of the pipe as opposed to the center. The average velocity, 9.65 m/s, was almost double that of the two and three mesh configurations. The final configuration for which data were collected across the full pipe diameter was carried out at a half-meter pipe length with the presence of a metal honeycomb. Again, for both honeycomb configurations, velocity versus diametral probe position was plotted as well as against the 1/7th power law (Figs.

9-10). At the 1/2 meter axial tunnel length, the profile showed a slight dip about the center, and the average velocity was lower than that of the 1 meter length (Table I). With an increase in pipe length from 1/2 meter to 1 meter, the profile distribution more closely followed the 1/7th power law.

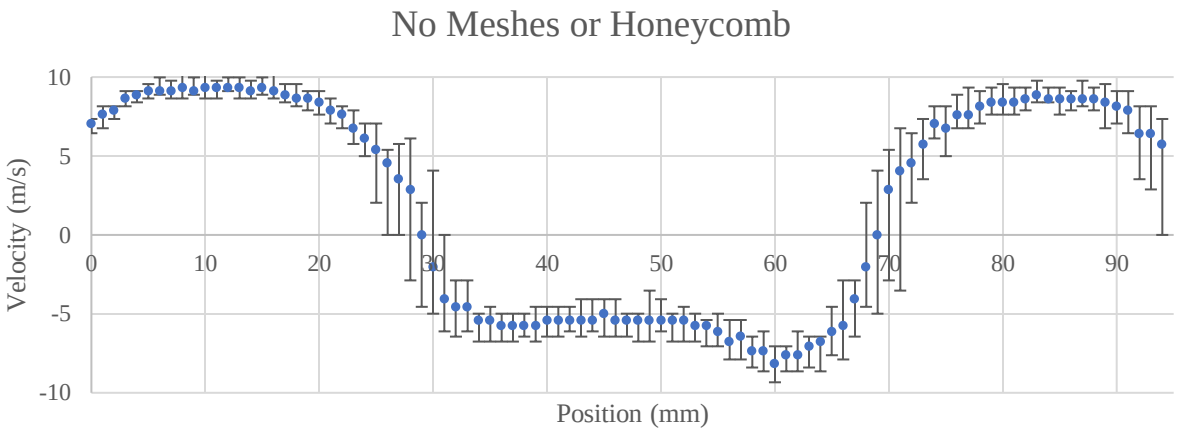

Fig. 4. Experimental velocity profile distribution with no means of flow correction and a pipe length of 1 meter.

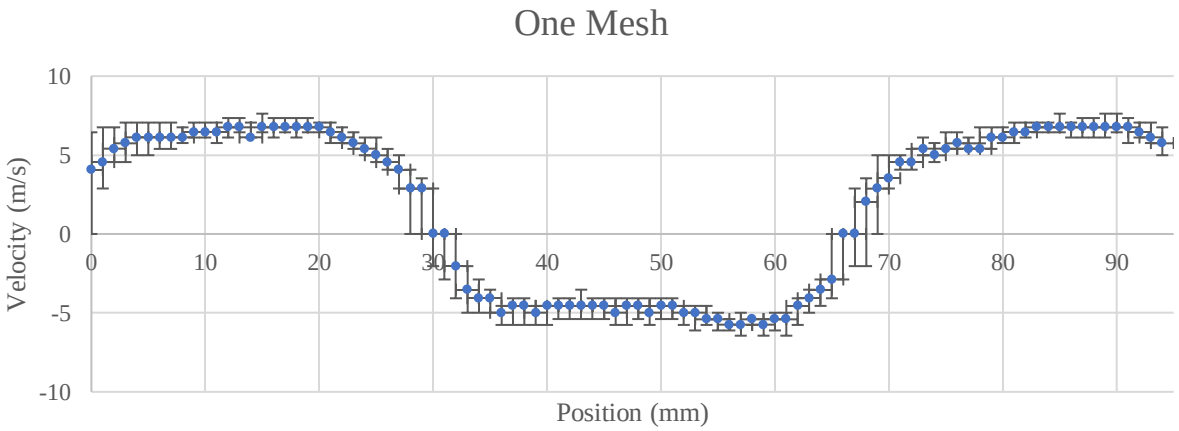

Fig. 5. Experimental velocity profile distribution with one mesh and a pipe length of 1 meter.

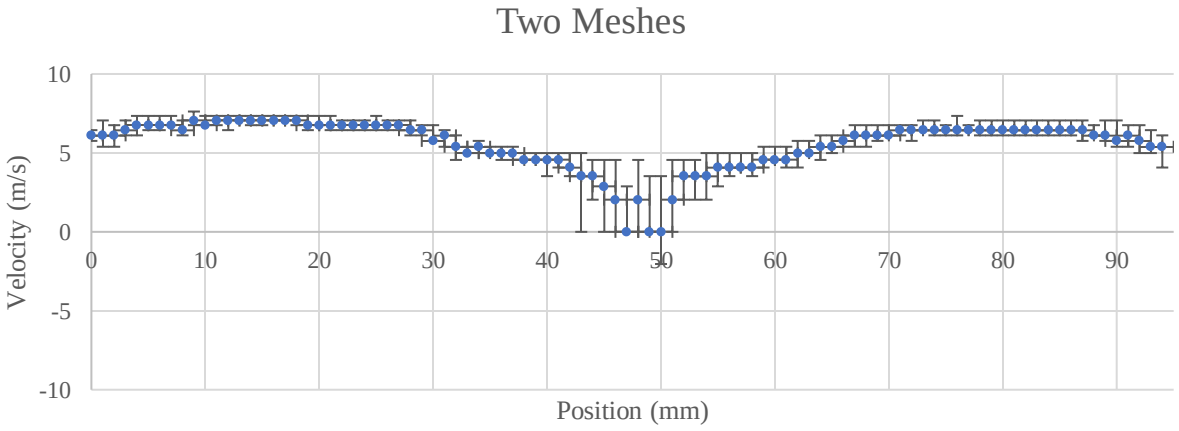

Fig. 6. Experimental velocity profile distribution with two meshes and a pipe length of 1 meter.

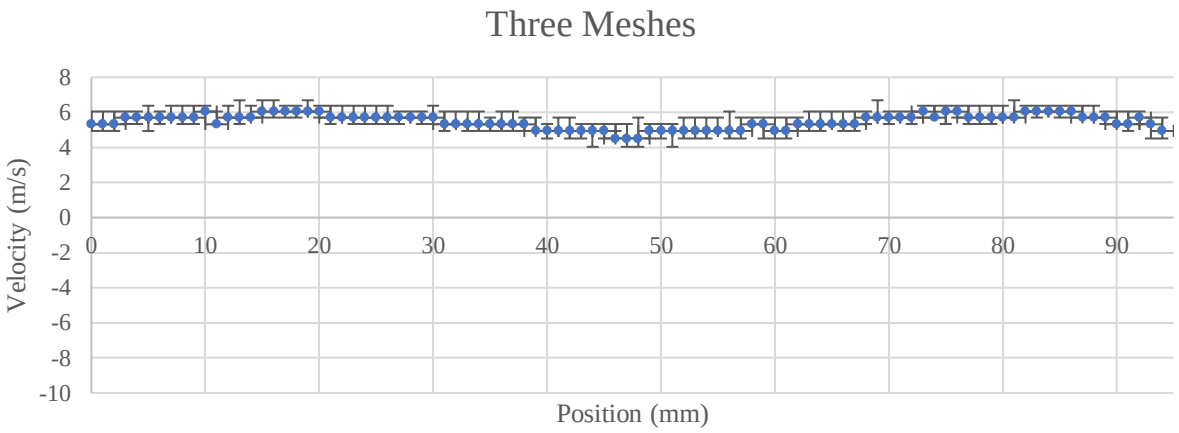

Fig. 7. Experimental velocity profile distribution with three meshes and a pipe length of 1 meter.

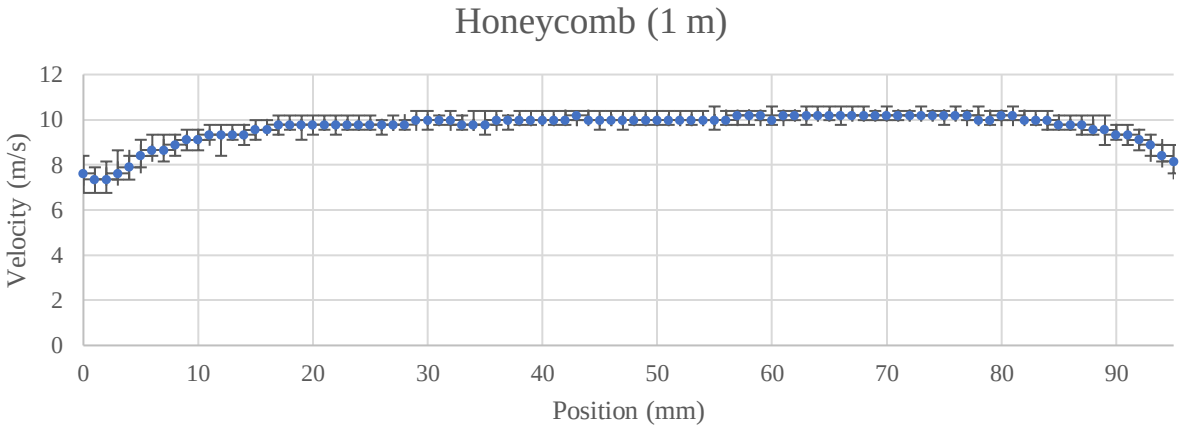

Fig. 8. Experimental velocity profile distribution with an aluminum honeycomb and a pipe length of 1 meter.

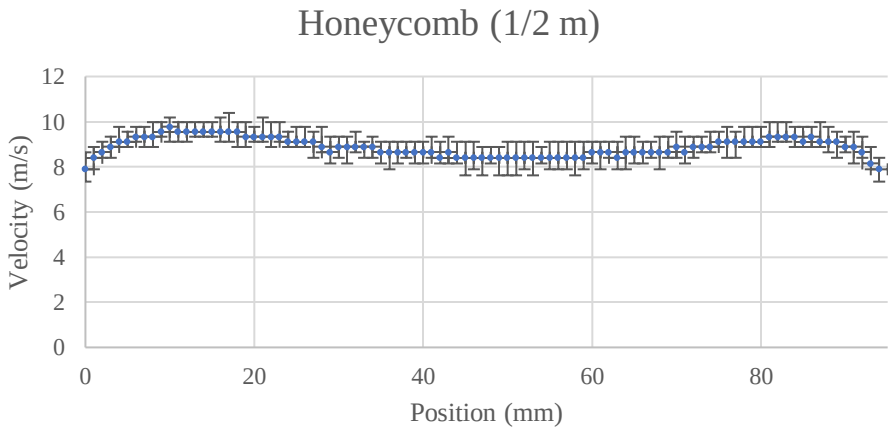

Fig. 9. Experimental velocity profile distribution with an aluminum and pipe length of ½ meter.

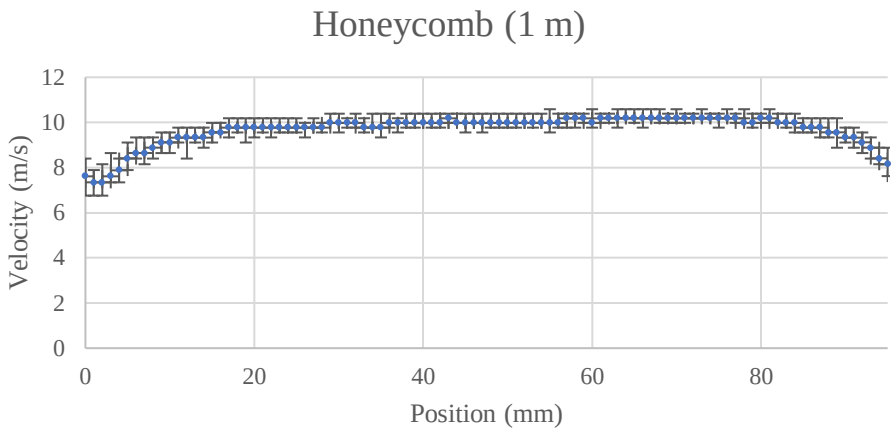

Fig. 10. Experimental velocity profile distribution with an aluminum honeycomb and a pipe length of 1 meter.

With the apparatus arranged vertically a ping pong ball was introduced, and observations noted (Fig. 11). With the presence of a single mesh, the ball traveled with circular motion touching the pipe walls near the opening of the pipe. Upon increasing the number of meshes, the ball followed the same path. However, it did so with decreasing velocity and at a further distance from the opening of the pipe. With the presence of the metal honeycomb, while the ball processed in a circular path, it did so at a much slower velocity. Moreover, it did not remain in the same plane when in motion. Rather it seemed to bob and float along its path moving above and below the opening of the pipe.

Fig. 11. Flow visualization technique through the introduction of a ping pong ball to the system.

Discussion

Due to the global pandemic forcing engineering lab courses online, there is an increased need for shippable hands-on remote laboratories for student use. The goal of this study was to characterize the initial prototype of a miniaturized wind tunnel to be used in such an application. This apparatus is intended to reinforce textbook theory associated with turbulent velocity profiles in pipes.

Investigation of the apparatus with flow driven by a computer fan revealed a central dead spot with negative core velocity. This effect was partially attributed to the fan's 51 mm hub, whose central placement and size closely mirrored the observed ~60 mm diameter dead spot in the middle of the flow field. As no flow is driven by the fan's hub, this fan component was linked to the decreased velocity measurements. More mysterious, however, was the presence of apparent negative velocity measurements in this dead spot. Given that flow is directed normal to the total pressure port and parallel to the static port, measurement of higher pressure (and thus higher velocity) at the static port was unexpected and presented a mystery!

Ultimately, this mysterious phenomenon was attributed to the presence of undesirable fluid axial spiraling (vorticity). This flow field induced an azimuthal velocity component as opposed to pure axial velocity as expected in textbook pipe flow. The azimuthal flow impinged on the pitot-static probe's static pressure port creating the illusion of a measured negative velocity. The azimuthal velocity component hypothesis was further supported when the ping pong ball was introduced to the vertical pipe system for flow visualization, and the ball precessed around the pipe (Fig. 11) revealing the azimuthal flow pattern.

Thus, the need for flow correction was realized and approached using screen meshes and a metal honeycomb. Increasing mesh numbers and finally placing honeycomb downstream of the fan successively reduced/mitigated the dead spot as demonstrated by improving minimum velocity readings with each successive correction. Again, this improvement is explained through reduced vorticity with each additional flow corrector and visualized using the ping pong ball. While the ping pong ball continued to follow a circular path, it did so at slower speed with each successive flow corrector following the measured vorticity trend.

For this apparatus and set of experiments, given the constant pipe radius and kinematic fluid density, Reynolds Number was solely dependent on the average flow velocity. Further, the fan speed and all other factors remained constant, aside from the means flow correction. Thus, the Reynolds Number was dictated by these correctors. The honeycomb facilitated the highest velocity flow. This is desirable as it allows the widest range of Reynolds Numbers to be investigated using the system. The presence of both two and three meshes provided the second highest average velocity, however, these values were still around half that the honeycomb provided.

Ultimately, the honeycomb was favored as the resulting velocity profile best reflected textbook turbulent profiles. It demonstrated the least vorticity in both the data and visualization technique, while also best maintaining velocity. Thus, the impact of pipe length was investigated using the honeycomb flow corrector. The 1-meter pipe better reflected the theoretical $1/7^{th}$ power law (Fig. 10) as compared to the 1/2-meter pipe length (Fig. 9). This investigation also revealed the presence of vorticity and recirculation in the flow at the 1/2-meter pipe length given the slight dead spot in the flow. However, this dead spot was not observed at the 1-meter pipe length. This explains the discrepancy between the average velocity measurements. According to mass conservation, the average velocity for both pipe lengths should be the same given their otherwise identical set up. Vorticity and recirculation effects in the half-meter pipe caused the decrease in apparent average velocity as the azimuthal velocity component cannot be directly detected by pitot-static probe. All these observations support pipe entry length theory, where velocity profiles develop further at longer lengths in the entry region.

Conclusion

An undergraduate mechanical engineering senior was mailed a prototype fluid mechanics teaching lab kit, and she evaluated it remotely to mimic conditions faced by a remote learner in an online lab class. Her only interactions were 1- to 2-hour weekly Zoom meetings with a faculty member. Despite the remote learning arrangement, this student observed and measured numerous engineering fluids phenomena relevant to a fluid dynamics course including velocity profile, flow

visualization, vorticity, and development length. Moreover, the student created and tested multiple kit design improvement while never setting foot inside a brick-and-mortar lab. This anecdotal experience shows that kit-based fluid mechanics instruction can be successfully implemented for remote learners at the undergraduate level.

Without flow correction, an unexpected dead spot was present in the velocity profile of the prototype kit configuration. This was attributed to the fan's hub and ultimately undesirable vorticity in the flow field. Addition of meshes and/or a metal honeycomb reduced these effects. The resultant honeycomb-corrected velocity profile shows strongest correspondence to the theoretical $1/7^{th}$ Power Law internal pipe flow velocity profile. Moreover, the best reflection of textbook turbulent velocity profile was observed at greater pipe lengths, reinforcing pipe entry length theory.

Most critically, *the underlying negative velocity mystery and its solution were realized because the kit was a hands-on experiment*. The problem would never have occurred in a computational fluid dynamics simulation with preset simple boundary conditions or, likewise, in a premanufactured laboratory-scale wind tunnel where vanes and straighteners eliminate flow rotation. While anecdotal, this experience illustrates how mailed experimental laboratory kits are critical to honing students' engineering skills. Moreover, it reinforces findings in the literature that remote learning can provide richer experiences than brick-and-mortar labs because students have freedom to explore interesting or unexpected phenomena without time limits imposed by laboratory periods in a brick-and-mortar setting. This work's key pedagogical conclusion is take-home kits are an important engineering teaching tool worth retaining after the global pandemic ends.

Currently, the kit allows students to investigate both flow correction and entry length. Future work will have an increased focus on kit modularity and include further flow characterization investigating the impact of pipe diameter and fan speed. It is also desirable for fully developed flow and the laminar flow to be achieved. Finally, the kit will be prototyped to minimize part cost, size, and weight to achieve the most affordable product.

References

1 ABET, "Accredited Programs – 100% Online Programs," [Online]. Available: https://amspub.abet.org/aps/online-search, accessed 1/28/2021

2 Fisher, Frank, Hamid Hadim, Sven Esche, Robert Ubell, and Constantin Chassapis, "Feasability of a Fully Online Undergraduate Mechanical Engineering Degree for Non-Traditional Learners," Annual Conference, American Society for Engineering Education, 2007.

3 Badiru, Adedeji, "A Vision For Engineering Education Post-Covid-19," Prism, American Society for Engineering Education, October 2020, pg. 13.

4 Auer, Michael and Christophe Gravier, "Guest Editorial: The Many Facets of Remote Laboratories in Online Engineering Education", IEEE Transactions on Learning Technologies, IEEE CS & ES, 2009, pg. 260-262.

5 Douglas, Jamie and Mark Holdhusen, "Development of Low-Cost, Hands-On Lab Experiements for Online Mechanics of Materials Course," Annual Conference , American Society for Engineering Education, 2013.

6 Corter, James, Sven Esche, Constantin Chassapis, Jing Ma, and Jeffrey Nickerson, "Process and learning outcomes from remotely-operated, simulated, and hands-on student laboratories," Computers and Education, Elsevier, 2011, pg. 2054-2067.

7 Corter, James, Jeffrey Nickerson, Sven Esche, Constantin Chassapis, Seogah Im and Jing Ma, "Constructing Reality: A Study of Remote, Hands-On, and Simulated Laboratories," ACM Transactions on Computer-Human Interaction, 2007.

8 Traum, Matthew and F. Hadi, "A Minituarized Circular Hydraulic Jump for Remote On-Line Fluid Mechanics Instruction," Journal of Online Engineering Education, 2019.

9 Samuelsen, Dag and Olaf Graven, "Remote Laboratories in Engineering Education - an Overview of Implementation and Feasibility," 14th LACCEI International Multi-Conference for Engineering, Education, and Technology, 2016.

10 "Flow in Pipes," Fluid Mechanics, [Online]. Available: https://www.kau.edu.sa/Files/0057863/Subjects/Chapter%208.pdf, 2004.

11 Muzychka, Y.S., "Internal Flows," ENGR 5961 Fluid Mechanics I, [Online]. Available: http://www.engr.mun.ca/muzychka/Fluids-Section-4.pdf.

12 "Critical Reynolds Number," Nuclear Power, [Online]. Available: https://www.nuclear-power.net/nuclear-engineering/fluid-dynamics/reynolds-number/critical-reynolds-number/.

13 White, Frank, Fluid Mechanics, Mcgraw-Hill, New York, 2011.

14 "Basics of internal forced convection," Thermal-Fluids Central. [Online]. Available: https://www.thermalfluidscentral.org/encyclopedia/index.php/Basics_of_internal_forced_convection, 2010.

15 "Entrance Length," University of Sydney Aerospace, Mechanical & Mechatronic Engg., [Online]. Available: http://www-mdp.eng.cam.ac.uk/web/library/enginfo/aerothermal_dvd_only/aero/fprops/pipeflow/node9.html, 2005.

16 "Pitot-Static Tube", NASA, [Online]. Available: https://www.grc.nasa.gov/WWW/K-12/airplane/pitot.html.

17 "Bernoulli's Equation," NASA [Online]. Available: https://www.grc.nasa.gov/WWW/K-12/airplane/bern.html.

Nina T. Jones

Nina T. Jones is a 4th-year mechanical engineering undergraduate student at UF. The research outlined in this paper was fueled by her efforts to obtain academic distinction via an Honors Thesis. In addition to this, Ms. Jones has academic research experience in chemistry and biomechanics; she fabricated a pen to electrolytically clean silver tarnish and investigated parametric models of the pelvis for crash simulation. She currently works as a contract engineer at Engineer Inc., a Gainesville education enterprise that designs and distributes STEM laboratory kits to remote learners. Her future goals include expanding and applying her skills in the aerospace field.

Sean R. Niemi

Sean R. Niemi is a Lecturer in the Department of Mechanical and Aerospace Engineering at UF, and founder of the MERGE (MEchanical engineeRing desiGn pEdagogy) Lab focusing his research and teaching efforts on Capstone Design, Mechanical Design, Design for Manufacturing, and Instrumentation Design. Sean co-advises the UF Rocket Team (Swamp Launch), mentoring a group of interdisciplinary students in developing a 10,000 ft. apogee rocket for the Intercollegiate Rocket Engineering Competition. He also mentors members of both the FSAE combustion and electric vehicle teams. Dr. Niemi has worked in industrial maintenance and aerospace, with graduate work in soft matter engineering, 3D bio-printing, and biotribology.

Matthew J. Traum

Matthew J. Traum is a Senior Lecturer in the Mechanical & Aerospace Engineering Dept. at UF. He is an experienced educator, administrator, and researcher with co-authorship of 62 peer-reviewed papers and over $865K in funding. In parallel to UF, Dr. Traum is CEO of Engineer Inc., a STEM education technology social enterprise that creates lab kits for distance and hybrid learners. Prior to UF, Dr. Traum was an Associate Professor and Director of Engineering Programs at Philadelphia University. He previously served on the MSOE ME faculty and co-founded the Mechanical & Energy Engineering Dept. at the University of North Texas. Traum received ME PhD/MS degrees from MIT, and he holds two BS from UC Irvine in ME and AE.